


## RESEARCH PAPER

# Magnesium therapy improves outcome in *Streptococcus pneumoniae* meningitis by altering pneumolysin pore formation

**Correspondence** Asparouh I. Iliev, MD, PhD, Institute of Anatomy, University of Bern, Baltzerstrasse 2, 3012 Bern, Switzerland.  
E-mail: asparouh.iliev@ana.unibe.ch

**Received** 10 March 2017; **Revised** 26 August 2017; **Accepted** 29 August 2017

Sabrina Hupp<sup>1,4,\*</sup>, Sandra Ribes<sup>2,3,\*</sup>, Jana Seele<sup>2,3,\*</sup>, Carolin Bischoff<sup>4</sup>, Christina Förtsch<sup>4</sup>, Elke Maier<sup>5</sup>, Roland Benz<sup>5</sup>, Timothy J Mitchell<sup>6</sup>, Roland Nau<sup>2,3</sup> and Asparouh I Iliev<sup>1,4</sup> 

<sup>1</sup>Institute of Anatomy, University of Bern, Bern, Switzerland, <sup>2</sup>Department of Neuropathology, University Medical Center Göttingen, Göttingen, Germany, <sup>3</sup>Department of Geriatrics, Evangelisches Krankenhaus Göttingen-Weende, Göttingen, Germany, <sup>4</sup>DFG Membrane/Cytoskeleton Interaction Group, Institute of Pharmacology and Toxicology & Rudolf Virchow Center for Experimental Medicine, University of Würzburg, Würzburg, Germany, <sup>5</sup>Rudolf Virchow Center for Experimental Medicine, University of Würzburg, Würzburg, Germany, and <sup>6</sup>Institute of Microbiology and Infection, College of Medical and Dental Sciences, University of Birmingham, Birmingham, UK

\*These authors contributed equally.

## BACKGROUND AND PURPOSE

*Streptococcus pneumoniae* is the most common cause of bacterial meningitis in adults and is characterized by high lethality and substantial cognitive disabilities in survivors. Here, we have studied the capacity of an established therapeutic agent, magnesium, to improve survival in pneumococcal meningitis by modulating the neurological effects of the major pneumococcal pathogenic factor, pneumolysin.

## EXPERIMENTAL APPROACH

We used mixed primary glial and acute brain slice cultures, pneumolysin injection in infant rats, a mouse meningitis model and complementary approaches such as Western blot, a black lipid bilayer conductance assay and live imaging of primary glial cells.

## KEY RESULTS

Treatment with therapeutic concentrations of magnesium chloride (500 mg·kg<sup>-1</sup> in animals and 2 mM in cultures) prevented pneumolysin-induced brain swelling and tissue remodelling both in brain slices and in animal models. In contrast to other divalent ions, which diminish the membrane binding of pneumolysin in non-therapeutic concentrations, magnesium delayed toxin-driven pore formation without affecting its membrane binding or the conductance profile of its pores. Finally, magnesium prolonged the survival and improved clinical condition of mice with pneumococcal meningitis, in the absence of antibiotic treatment.

## CONCLUSIONS AND IMPLICATIONS

Magnesium is a well-established and safe therapeutic agent that has demonstrated capacity for attenuating pneumolysin-triggered pathogenic effects on the brain. The improved animal survival and clinical condition in the meningitis model identifies magnesium as a promising candidate for adjunctive treatment of pneumococcal meningitis, together with antibiotic therapy.

## Abbreviations

CDC, cholesterol-dependent cytolysin; CFU, colony-forming unit; HU, haemolytic unit; PI, propidium iodide; PLY, pneumolysin; PSD95, postsynaptic density 95

## Introduction

*Streptococcus pneumoniae* (pneumococcus) is a common bacterial pathogen that causes meningitis in humans, accompanied by high lethality (~30%) and substantial cognitive disabilities in survivors (Koedel *et al.*, 2002). Pneumolysin (PLY), a member of the cholesterol-dependent cytolysin (CDC) group and a major pneumococcal neurotoxin, is one of the key pathogenic factors that causes deterioration over the course of *S. pneumoniae* meningitis (Wellmer *et al.*, 2002) and pneumococcal lung infections (Canvin *et al.*, 1995). PLY produces pores and cell lysis at high concentrations and non-lytic changes at lower concentrations (Iliev *et al.*, 2007; Iliev *et al.*, 2009). The CDC protein family includes toxins from Gram-positive bacteria that share a common dependence on the presence of cholesterol in cell membranes (Alouf, 2000). PLY-expressing pneumococcal strains cause more severe disease than PLY-negative strains (Reiß *et al.*, 2011), and the concentration of PLY in the CSF of patients with meningitis correlates with the outcome (Wall *et al.*, 2012).

PLY, which has been thoroughly studied ultrastructurally in artificial membranes (Tilley *et al.*, 2005), produces pores by first binding to membrane cholesterol, aligning in arcs and forming pre-pore structures of 30–50 monomers, followed by molecular unfolding and membrane perforation producing 26–30 nm wide lytic pores. The toxin comprises four domains: domain 4 mediates binding to membrane cholesterol, while domains 1, 2 and 3 establish the pre-pore barrel. Upon alignment in a ring-shaped pre-pore, domain 3 refolds into two  $\beta$  hairpins (each containing two parallel  $\beta$  strands), which penetrate the membrane and build the internal  $\beta$  barrel of the pore (Tilley *et al.*, 2005). The artificial membrane ultrastructural studies utilize mostly concentrations of  $2 \mu\text{g}\cdot\text{mL}^{-1}$  PLY and higher. In the CSF of patients with meningitis, however, the concentrations of PLY do not exceed  $0.2 \mu\text{g}\cdot\text{mL}^{-1}$ , which is mildly lytic in cell cultures and non-lytic in tissue culture systems (Spreer *et al.*, 2003; Iliev *et al.*, 2007; Iliev *et al.*, 2009). We shall call such concentrations sublytic. We have shown before that sublytic concentrations of PLY produce cytoskeletal changes, including actin remodelling and microtubule stabilization, without plasmalemmal permeabilization (Iliev *et al.*, 2007; Iliev *et al.*, 2009). The short-term (within a few hours) effects of PLY involve interstitial tissue oedema and increased pathogen tissue penetration in the brain, both caused by astrocyte remodelling (Hupp *et al.*, 2012).

The management of bacterial meningitis involves corticosteroids as adjuvants to prevent fatal oedema (Grandgirard and Leib, 2010) and includes antibiotics. The administration of bactericidal, but non-bacteriolytic, antibiotics has proved to reduce lethality and sequelae more effectively than bacteriolytic antibacterials, most likely due to the reduced concomitant release of neurotoxic factors such as PLY (Nau *et al.*, 1999; Spreer *et al.*, 2003; Grandgirard *et al.*, 2012). However, the bacteriolytic family of  $\beta$ -lactam antibiotics still constitutes the standard treatment, and no efficient and clinically applicable therapy exists to counteract the detrimental effects of PLY already released into the compartments of the CNS.

In this work, we have demonstrated that clinically relevant concentrations of **magnesium (as  $\text{Mg}^{2+}$ )** decrease

most of the tissue pathogenic effects of PLY and improve the outcome of pneumococcal meningitis in animal models of the disease.

## Methods

### *Pneumolysin preparation*

Wild-type PLY was expressed in *Escherichia coli* BL-21 cells (Stratagene, Cambridge, UK) and purified by metal affinity chromatography as described previously (Douce *et al.*, 2010). The purified PLY was evaluated for the presence of contaminating Gram-negative LPS using the colorimetric LAL assay (KQCL-BioWhittaker, Lonza, Basel, Switzerland). All purified proteins showed  $<0.6$  endotoxin units per  $\mu\text{g}$  protein. The stock of purified wild-type toxin exhibited an activity of  $2 \times 10^4$  haemolytic units (HUs) per mg. In all experiments, cells and tissues were treated with PLY in serum-free medium.

### *Cell and slice cultures, vital staining, live imaging and treatments*

Primary glial cultures (astrocytes and microglia) were prepared from the brains of postnatal day (P) 4–6 of either C57BL/6 mice (Janvier Labs, Le Genest-Saint-Isle, France) or Sprague Dawley (SD) rats (Charles River WIGA GmbH, Germany) as previously described (Iliev *et al.*, 2004) in DMEM (Life Technologies, Thermo Fisher Scientific, Schwerte, Germany) supplemented with 10% fetal calf serum (PAN Biotech GmbH, Aidenbach, Germany) and 1% penicillin/streptomycin (Life Technologies) in  $75 \text{ cm}^2$  poly-L-ornithine- (Sigma-Aldrich Chemie GmbH, Schnellendorf, Germany)-coated cell culture flasks (Sarstedt AG & Co., Nuembrecht, Germany). The total number of animals used for primary cultures was 10, and they were killed by decapitation [an approved method in the German Animal Protection Law (Tierschutzgesetz)].

Acute brain slices were prepared from P10–14 C57BL/6 mice (12 animals) or SD rats (12 animals) by decapitation. This method provides brain tissue in optimal conditions for acute brain slices by vibratome sectioning (Vibroslice NVSL, World Precision Instruments, Berlin, Germany) in Basal Medium Eagle (BME; Life Technologies), continuously oxygenated with carbogen gas (95%  $\text{O}_2$ , 5%  $\text{CO}_2$ ) at  $4^\circ\text{C}$ . The slices were allowed to adapt in carbogenated BME with 1% penicillin/streptavidin and 1% glucose at  $37^\circ\text{C}$  for 1 h before being challenged with PLY under the same conditions. In these acute slices, cell lysis never exceeded 5% within 12 h (as judged by an LDH release test).

In tissue remodelling experiments, the acute slices were incubated with 70 kD dextran-TRITC (Life Technologies,  $0.5 \text{ mg}\cdot\text{mL}^{-1}$ ) for 10 min at  $37^\circ\text{C}$  before fixation with 2% paraformaldehyde (Carl Roth GmbH, Karlsruhe, Germany) in PBS to assess molecular penetration. The fixed samples were examined by scanning confocal microscopy on a Leica LSM SP5 (Leica Microsystems Heidelberg GmbH, Mannheim, Germany) followed by 3D reconstruction of the z-stacks (1  $\mu\text{m}$  scanning step) and measurement of penetration using ImageJ software (version 1.43 g for Windows OS, National Institute of Health, Bethesda, Maryland, USA).

For live imaging experiments, the cells were incubated at 37°C in CO<sub>2</sub>-insensitive L-15 Leibovitz's medium (Life Technologies) containing propidium iodide (PI) to stain permeabilized cells, and Hoechst 33 342 to stain the nuclei of all cells (1 µg·mL<sup>-1</sup>; Life Technologies). The cells were visualized on an Olympus Cell-M Imaging system using the 10× and 20× dry objectives (Olympus Deutschland GmbH, Hamburg, Germany). LDH release assays were performed using CytoTox96 non-radioactive cytotoxicity assay according to manufacturer's instructions (Promega, Madison, WI, USA).

### *Animal procedures and choice of animal models*

All animal care and experimental procedures were performed according to the regulations of the German Research Animal Protection Law (Tierschutzgesetz) with approval from the Commission for Animal Experiments Government of Lower Franconia, Bavaria, Germany, and approval from the Authority for Consumer Protection and Food Safety of Lower Saxony [Niedersächsisches Landesamt für Verbraucherschutz und Lebensmittelsicherheit (LAVES)], Braunschweig, Lower Saxony, Germany. Animal studies are reported in compliance with the ARRIVE guidelines (Kilkenny *et al.*, 2010; McGrath and Lilley, 2015).

All animals were maintained for 1 week before the start of the experiments in an animal facility with 12/12 h light/dark cycles and water and food *ad libitum*. All experiments were terminated in such a way as to avoid animal suffering. Animal experiments were performed in two different animal species systems (mice and rats) to increase cross-species translational relevance. The choice of the most suitable animal model for experiments represents a major task that has to be considered carefully. Ample evidence indicates the risk of misleading interpretations when using only one species model or model that is not at correct age, correct condition or susceptible to disease (Denayer, Stöhr, and Van Roy, 2014). The most widely used experimental animal model species are rats and mice, and despite being wrongly considered similar, they are actually separated by 12–24 million years of evolution and differ substantially (Blanga-Kanfi *et al.*, 2009). Thus, the confirmation of therapeutic effect simultaneously in both species increases substantially the chance of translational value to humans. At the same time, the current legal and bioethical standpoint strongly urges researchers to reduce the number of experimental animals, especially when experimental models are accompanied with potentially higher level of suffering (Flecknell, 2002). To accommodate both issues, we chose to verify the effects of magnesium in two live animal models – SD rats and C57Bl/6 mice, testing the role of magnesium on pure toxin in one of them only and the effect in full-scale disease in the other.

### *Preparation of animal models*

For induction of PLY-based animal brain swelling, 29 infant SD rats (P10–14) were used. The choice of the model was based on our earlier experience that showed more efficient i.c.v. toxin distribution in the ventricular system of rats, than in mice, when toxin-induced swelling was studied (Hupp *et al.*, 2012). Rats were randomly distributed to form the following groups: i.c.v. saline-injected mock control ( $n = 9$ ), i.c.v. PLY-injected group ( $n = 11$ ) and magnesium (500 mg·kg<sup>-1</sup>) pretreated and subsequently i.c.v. PLY-injected group ( $n = 9$ ). The animals were anaesthetized with

ketamine/xylazine (s.c., ketamine, 80 mg·kg<sup>-1</sup>; xylazine, 12 mg·kg<sup>-1</sup>; Sigma), with follow-up anaesthesia using ketamine (s.c., 30 mg·kg<sup>-1</sup>·h<sup>-1</sup>). During the experiments, the blood pressure and the pulse frequency of each anaesthetized animal were monitored by a non-invasive tail measurement system (Stoelting Co., Wood Dale, IL, USA) to confirm proper physiological conditions. To confirm the pathophysiological relevance of the injected amounts, samples from the CSF were taken within 2 h of the injection of PLY and/or 1% Evans Blue dye (Sigma) to show the complete distribution of the injected fluid in the CSF. The final concentration of PLY was 0.2 µg·mL<sup>-1</sup> (Wippel *et al.*, 2011), which was comparable to the toxin amounts observed in the CSF during pneumococcal meningitis (Spreer *et al.*, 2003). Equimolar amounts of albumin Fr. V (Sigma) were applied instead of PLY in control animals.

For induction of bacterial meningitis, 44 two-month-old female C57Bl/6 mice were used according to an established protocol, used frequently in this research field (Nau *et al.*, 1999). Mice received an intracerebral (i.c.) injection of either 10 µL containing  $1 \times 10^5$  colony-forming unit (CFU)·mL<sup>-1</sup> (1000 CFU per mouse) of *S. pneumoniae* D39 in saline ( $n = 37$ ) or 10 µL of sterile saline ( $n = 7$ ) after i.p. anaesthesia with ketamine (100 mg·kg<sup>-1</sup>) and xylazine (10 mg·kg<sup>-1</sup>) (Wellmer *et al.*, 2002). The health status of the mice was assessed every 12 h by a clinical score [0, no apparent behavioural abnormality; 1, moderate lethargy (apparent decrease of spontaneous activity); 2, severe lethargy (rare spontaneous movements, but walking after stimulation by the investigator); 3, unable to walk; 4, dead] (Gerber *et al.*, 2001), and the AUCs of the clinical scores were calculated for each animal. As a consequence of the muscle-relaxant effect of Mg<sup>2+</sup>, animals receiving MgCl<sub>2</sub> were susceptible to an inhibition of ventilation by anaesthetics. To avoid negative potentiation of ventilation inhibition, MgCl<sub>2</sub> administration was delayed to 30 min after induction of anaesthesia. To limit the number of injections, animals were treated with three doses (every 12 h, starting 30 min before i.c.v. injection) of a 0.33 mL solution containing either 30.45 mg MgCl<sub>2</sub>·mL<sup>-1</sup> or 0.33 mL of 0.45% saline i.p. Animals were treated i.p. with 0.33 mL solution of 30.45 mg MgCl<sub>2</sub>·mL<sup>-1</sup> or 0.33 mL of 0.45% saline. Solutions of MgCl<sub>2</sub>·6H<sub>2</sub>O were made in 0.45% saline. As the MgCl<sub>2</sub>-dependent effect was only observed until 12 h after the last MgCl<sub>2</sub> treatment, mice were killed under anaesthesia 36 h after infection by cervical dislocation. This time point was also defined to reduce excessive suffering of the animals when reaching 50% lethality. Blood samples, spleen and cerebellum were collected, plated and cultured on blood agar. The cerebrum was fixed in 4% formalin, dehydrated and paraffin-embedded for further processing and analysis (cutting and immunohistochemistry).

### *Animal group sizes, randomization, blinding and normalization*

The number of experimental animals used was kept to a minimum by statistical optimization in accordance with Altman's nomogram (O'Hara, 2008). The exact number of animals in different groups is indicated either in the figure legends or in the Methods section. The total number of animals used in all experiments was 113 (107 in the

experimental series, 3 for adjustment of the anaesthesia and 3 for preliminary analysis of optimal magnesium concentration). All animals were randomized before treatment. In all animal experiments and in all further sample analyses, the animals and samples were not identified before evaluation (blinded) and un-blinded upon statistical analysis. Normalization versus control groups (mock-treated and magnesium-treated controls) was employed in histological analysis of postsynaptic fluorescence intensity to correct for intensity staining changes, by the treatment with magnesium.

### Oedema evaluation

For the analysis of brain swelling, 10  $\mu\text{L}$  of 1% Evans Blue dye was injected i.c.v. 6 h after the first injection (mock or PLY), and the needle was kept in place for an additional 30 min, completely sealing the tiny skull opening. Within this time, nearly all dye was redistributed in the CSF. As the intracranial pressure increased, larger amounts of the dye/CSF mix would leak out after needle removal to equilibrate the pressure. The dye was absorbed onto filter paper, and the size of the spot, which was proportional to the total amount of fluid, was scanned and measured (in  $\text{mm}^2$ ) with ImageJ. This method for oedema evaluation was better than others when working with infant rodents (Hupp *et al.*, 2012). During the whole procedure, all animals were maintained under anaesthesia without interruption and at the end were killed by cervical dislocation.

The water content of the brain slices was analysed by specific gravity (also known as relative density) measurement in a Percoll (Sigma) density gradient (Tengvar *et al.*, 1982). The gradient ranged from 1.065 to 1.009 and was produced by dilution of isotonic Percoll in PBS (10:1 Percoll: 10 $\times$  PBS), thus creating 21 layers in increments of 0.0025. Oedematous tissue demonstrates a decreased relative density due to its increased water content, so it floats in a Percoll layer with a lower relative density.

### Immunohistochemistry

For the immunohistochemical experiments, microtome slices from mouse brains embedded in paraffin were deparaffinized and rehydrated, and the antigen was unmasked using target retrieval solution (Dako Deutschland GmbH, Hamburg, Germany) at 95°C. The primary antibodies used were rabbit anti-PSD95 (1:500; Abcam, Cambridge, UK) and rabbit anti-active caspase-3 (1:250; RnD Systems, Bio-Techne AG, Zug, Switzerland), and the secondary antibodies were goat anti-rabbit tagged with FITC or Cy3 (1:200; Dianova GmbH, Hamburg, Germany). Isotype controls confirmed the specificity of the staining. The sample nuclei were stained with DAPI (4,6-diamidino-2-phenylindole dihydrochloride, 1  $\mu\text{g}\cdot\text{mL}^{-1}$  in PBS; Life Technologies). All samples were preserved with the ProLong antifade reagent (Life Technologies).

### Protein biochemistry

Equal number of cells (500 000 per 60 mm Petri dish) were challenged either with PLY alone or in the presence of additional 2 mM  $\text{Mg}^{2+}$  for 15 min at 37°C in serum-free medium. Cells were washed three times with ice-cold PBS before proceeding further. Total crude cell membranes were isolated as described before (Iliev *et al.*, 2007). Shortly, cells were homogenized in buffer containing 10 mM Tris HCl (pH 7.4),

1 mM EDTA, 200 mM sucrose (all from Sigma-Aldrich) and protease inhibitor mix (Roche Diagnostics, Mannheim, Germany). The nuclei and cellular debris were removed by centrifugation at 900 $\times$  g for 10 min at 4°C. The resulting supernatant was centrifuged at 110 000 $\times$  g for 75 min at 4°C. Part of this supernatant was used for actin protein control samples for the Western blots. The crude membrane pellet was solubilized in buffer containing 10 mM Tris HCl (pH = 7.4), 1 mM EDTA, 0.5% Triton X-100 and protease inhibitor mix and boiled in Laemmli buffer at 95°C for 20 min.

Samples containing equal amounts of protein (BCA test, Thermo Fisher) were loaded on a nitrocellulose membrane (Schleicher & Schuell GmbH, Dassel, Germany) using a Novex® Tris-Glycine polyacrylamide gel system (Life Technologies). After semi-dry blotting, the membranes were blocked with 5% non-fat milk and incubated with rabbit anti-PLY antibody (Abcam Inc.; 1:400) and mouse anti-actin antibody (Sigma; 1:1000) as a loading control. After incubation with a horseradish peroxidase-conjugated goat anti-mouse and goat anti-rabbit secondary antibodies (Dianova), the bands were visualized using an ECL kit (GE Healthcare, Munich, Germany).

### Planar (black) lipid bilayer experiments

The planar lipid bilayer experiments were carried out as previously described (Benz *et al.*, 1978). Membranes were formed from a 1% (w/v) solution of oxidized cholesterol in n-decane (Sigma). This artificial lipid was used instead of diphytanoyl phosphatidylcholine because it facilitates the insertion of porin and PLY pores into the lipid bilayer (Benz *et al.*, 1980). The toxin (0.5  $\mu\text{g}\cdot\text{mL}^{-1}$ ) was added to the aqueous phase after the membrane had turned black. The membrane current was measured with a pair of Ag/AgCl electrodes with salt bridges switched in series by a voltage source and a highly sensitive current amplifier (Keithley 427, Keithley Electronics, Garland, TX, USA) in a buffer containing 100 mM KCl, 10 mM HEPES and various concentrations of  $\text{MgCl}_2$ . The temperature was maintained at 20°C throughout the experiment.

### Evaluation of data and statistical analysis

The data and statistical analysis comply with the recommendations on experimental design and analysis in pharmacology (Curtis *et al.*, 2015). Image processing and image analysis were performed using ImageJ software, version 1.43g for Windows. All values in the graphs represent mean  $\pm$  SEM. Statistical analyses were performed on GraphPad Prism 4.02 for Windows (GraphPad Software Inc., La Jolla, CA, USA). Statistical tests included the Mann-Whitney *U*-test (comparing two groups, varying one parameter at a time), one-way ANOVA with a Bonferroni post test (comparing three or more groups, varying one parameter at a time) and the log-rank test to compare survival between two groups. When non-linear regression analysis was performed, one-phase exponential association was used. For all analyses, we considered values of  $P < 0.05$  as statistically significant.

### Nomenclature of targets and ligands

Key protein targets and ligands in this article are hyperlinked to corresponding entries in <http://www.guidetopharmacology.org>, the common portal for data from

the IUPHAR/BPS Guide to PHARMACOLOGY (Southan *et al.*, 2016), and are permanently archived in the Concise Guide to PHARMACOLOGY 2015/16 (Alexander *et al.*, 2015a,b).

## Results

### Magnesium diminishes interstitial brain oedema by pneumolysin

Interstitial brain oedema caused by PLY represents a tissue-specific, toxin effect (Hupp *et al.*, 2012). Here, brain swelling was quantified using the reduction of the relative density in an acute brain slice culture model system. We used concentrations of PLY corresponding to  $4 \text{ HU}\cdot\text{mL}^{-1}$ , which were non-lytic but produced oedema in slices (Hupp *et al.*, 2012). First, the effects of therapeutic concentrations of  $\text{Mg}^{2+}$  (0.5–2 mM) on PLY-induced tissue swelling were investigated. The basal medium in all experiments contained 2.5 mM  $\text{Mg}^{2+}$ , and  $\text{MgCl}_2$  was added to the basal medium to reach therapeutic concentrations. In all experiments, the notation ‘without Mg’ means without additional  $\text{Mg}^{2+}$  above the basal medium concentration of 2.5 mM. Addition of 2 mM  $\text{Mg}^{2+}$  completely blocked the brain oedema produced after 6 h of  $4 \text{ HU}\cdot\text{mL}^{-1}$  PLY exposure (Figure 1A). Magnesium-induced prevention of brain swelling was concentration-dependent (Figure 1B). Because PLY allows deeper penetration of whole pneumococci and bacterial products into the tissue due to wider intercellular spaces (Hupp *et al.*, 2012), we quantified penetration using incubation with a fluorescently labelled dextran (MW = 70 kD). Again, the addition of 2 mM  $\text{Mg}^{2+}$  fully restored the normal permeability of the tissue when applied simultaneously with PLY and diminished the penetration of dextran to control values (Figure 1C).

Next, we tested whether the beneficial effects of magnesium were due to (i) tissue conditioning, (ii) modulation of the interaction of the toxin with the tissue or (iii) the effect

on the toxin alone. First, slices were pre-incubated with high concentrations of  $\text{Mg}^{2+}$  for 1 h before the toxin was added to the medium (PLY + Mg) (Figure 2A). Tissue swelling was completely prevented. Next, we exposed slices to PLY and  $\text{Mg}^{2+}$  without tissue pretreatment with  $\text{Mg}^{2+}$  (PLY and Mg). The beneficial effect of  $\text{Mg}^{2+}$  was preserved again (Figure 2A). In the third approach, slices were pre-treated with  $\text{Mg}^{2+}$  for 1 h, then  $\text{Mg}^{2+}$  was removed and PLY added (group Mg→PLY). Here, the pretreatment with  $\text{Mg}^{2+}$  was ineffective against PLY-induced brain oedema (Figure 2A). Altogether, this demonstrated that the action of Mg was most prominent when applied on the tissue together with PLY, and we concluded that  $\text{Mg}^{2+}$  exerted its effect by modulating toxin/cell interactions. Pre-incubation of the toxin together with high concentrations of  $\text{Mg}^{2+}$  for 1 h followed by slice challenge in basal medium without additional  $\text{Mg}^{2+}$  was partially effective against toxin-induced oedema (Figure 2B), indicating some effect limited to the toxin only.

### Magnesium diminishes the pore-forming capacity of pneumolysin

To analyse whether the elevation of  $\text{Mg}^{2+}$  in the medium affects the binding of PLY to the cell membrane, we performed Western blot analysis on the membrane fraction from glial cells after challenge with PLY. No decrease in the toxin binding in primary glial cells was observed 15 min after challenge (Figure 3A and Figure S2). Next, we measured the conductance of the PLY pores in black lipid membranes in the presence or absence of  $\text{Mg}^{2+}$  to detect alterations in pore structure. No change in the conductance profile was observed in the conductance event frequency histograms with similar peak conductance around 25 nS (Figure 3B). We studied the permeabilization of primary glia in culture by PLY in the presence and absence of additional  $\text{Mg}^{2+}$ . The concentrations that are pro-oedematous and non-lytic in slices are partially lytic in dissociated primary glial cultures (up to 10%, we call them sublytic), and this can be analysed by PI permeabilization. Additional  $\text{Mg}^{2+}$  significantly

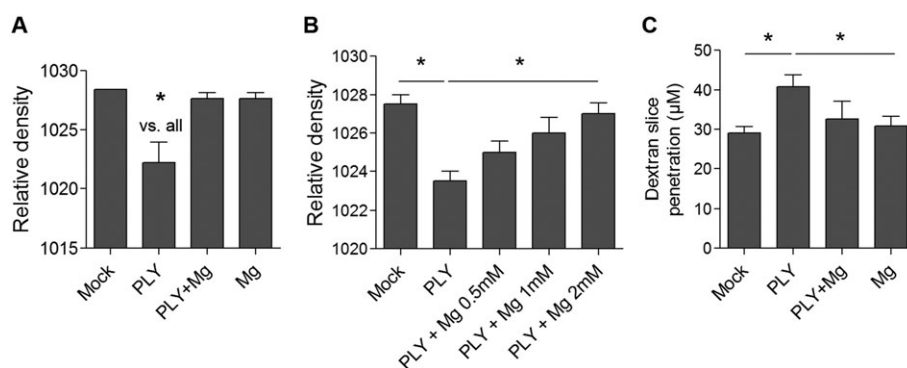


## Figure 1

*Ex vivo* inhibition of PLY-induced swelling by  $\text{MgCl}_2$ . (A) Relative density (lower density indicates higher water content and swelling) of brain slices after 6 h incubation without treatment (mock), with exposure to  $4 \text{ HU}\cdot\text{mL}^{-1}$  PLY, treatment with 2 mM Mg only (Mg) or combined exposure to PLY and Mg ( $n = 6$  independent experiments). (B) Concentration-dependent inhibition by  $\text{Mg}^{2+}$  of rat brain swelling after 6 h co-exposure of  $4 \text{ HU}\cdot\text{mL}^{-1}$  PLY ( $n = 5$  independent experiments). (C) Effect of 2 mM Mg to  $4 \text{ HU}\cdot\text{mL}^{-1}$  PLY on penetration of dextran-TRITC in rat brain slices ( $n = 5$  independent experiments). \* $P < 0.05$ , significantly different as indicated.

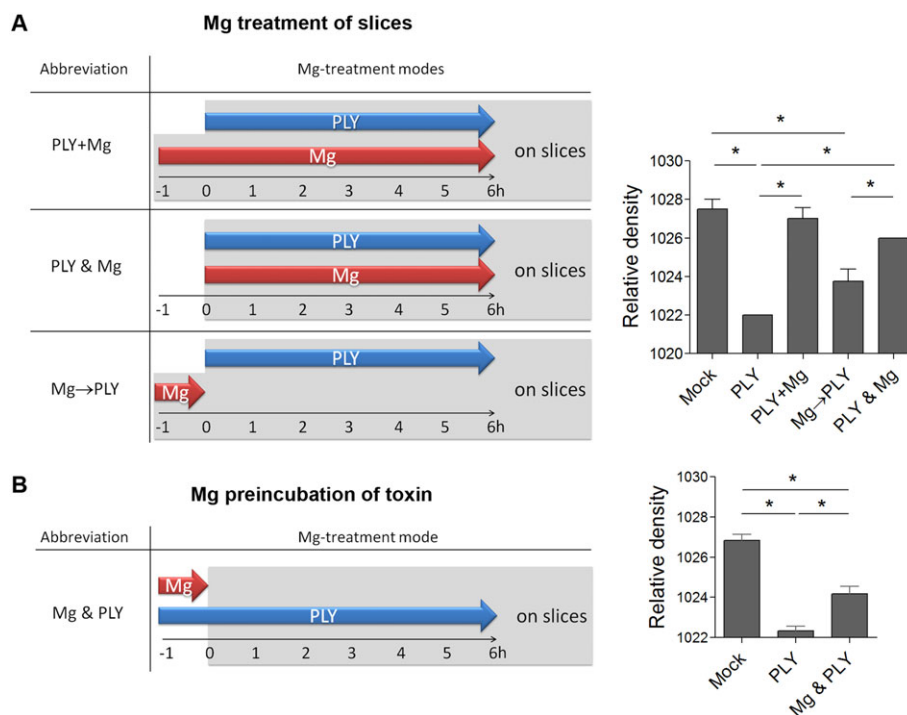


**Figure 2**

Attenuation of brain swelling by different schedules for magnesium application. (A) Schematic diagram of the different modes of magnesium (Mg) application (left). Inhibition of PLY-induced oedema by 4 HU·mL<sup>-1</sup> for 6 h by simultaneous incubation with 2 mM Mg<sup>2+</sup> with 1 h pre-incubation of the slices with Mg<sup>2+</sup> (PLY + Mg) and without slice pre-incubation (PLY and Mg). Pre-incubation of the slices with Mg<sup>2+</sup> for 1 h and removal before adding PLY (Mg→PLY) did not alter toxin-triggered oedema ( $n = 5$  independent experiments). (B) Partial inhibition of rat brain slice swelling by pre-incubation of PLY with 2 mM Mg<sup>2+</sup> for 1 h, followed by treatment of slices in normal medium without additional Mg<sup>2+</sup> with 4 HU·mL<sup>-1</sup> PLY for 6 h ( $n = 5$  independent experiments). \* $P < 0.05$ , significantly different as indicated.

delayed the permeabilization of glial cells by PLY (Figure 3C, D) with differences in the permeabilization endpoints after regression analysis curve extrapolation as well (Figure 3E). Assay of cytotoxicity based on LDH release confirmed these findings. Five hours after toxin challenge in cell culture, however, the cytotoxicity of toxin-challenged groups (both with and without additional Mg<sup>2+</sup>) was equal (Figure 3F). Thus, Mg<sup>2+</sup> delayed pore formation by PLY without modulation of binding and conductance profile of the pores. All experiments were carried out both in SD rats and C57BL/6 mouse cell systems with similar outcomes.

### Inhibition of brain swelling by pneumolysin in animals

Next, we tested whether the systemic application of Mg may be a suitable therapeutic alternative in whole-animal paradigms. We tested two different species systems to increase the translational relevance of our findings. Intracerebroventricular injection of PLY (at a final concentration of 4 HU·mL<sup>-1</sup>) into the CSF of young rats (P10–14) produced brain oedema as evaluated by the Evans blue method, following an established protocol (Hupp *et al.*, 2012). Pretreatment with Mg<sup>2+</sup> (500 MgCl<sub>2</sub>·6H<sub>2</sub>O·kg<sup>-1</sup> i.p.; dose was determined by extrapolation of the results from brain slices experiments to animals considering volume of distribution, effects of serum Mg<sup>2+</sup> elevation on CSF Mg

concentration and preliminary tests in single animals) significantly reduced the amount of brain swelling in the infant rats 6 h after toxin challenge (Figure 4). This dose of Mg<sup>2+</sup> demonstrated some muscle relaxation in treated animals under anaesthesia as determined by decreased muscle tonus.

### Improved survival, synaptic loss and clinical status in meningitis animals

Finally, we investigated the role of Mg<sup>2+</sup> as a potential treatment in the mouse model of pneumococcal meningitis that has been widely used in the field (Nau *et al.*, 1999). No differences in bacterial titers in spleen, cerebellum and blood (Figure 5A) and in weight loss (Supporting Information Figure S1A) were observed between mock and magnesium-treated infected animals at the end of the experiment. The predefined endpoint for analysis of lethality was 36 h (see Methods). Immunohistochemically, we analysed synapses in layers I–III of the neocortex by PSD95 (a postsynaptic marker) immunostaining. The analysis revealed that treatment with Mg<sup>2+</sup> blocked the loss of PSD95 immunostaining at 36 h after infection with *S. pneumoniae* (Figure 5B). No significant differences in the elevated number of cells positive for active **caspase-3** in the CA2 area of the hippocampal formation were observed between the two groups of infected mice (Supporting

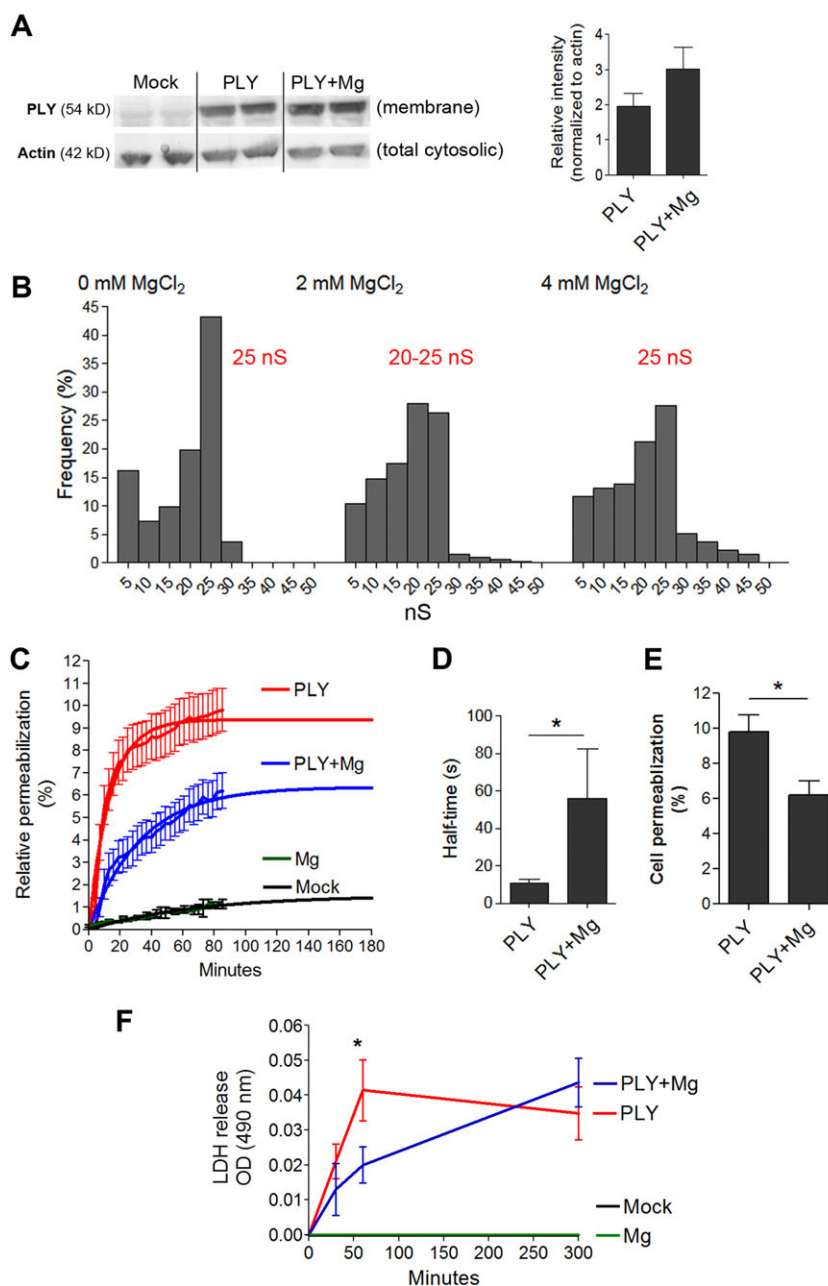


### Figure 3

Mechanisms of modulation of PLY properties by magnesium. (A) The presence of  $Mg^{2+}$  does not inhibit toxin binding to mouse glial cells (Western blot) 15 min after challenge with  $4 \text{ HU} \cdot \text{mL}^{-1}$  (4 independent experiments). (B) The conductance profile of PLY in a black lipid bilayer demonstrates an unchanged conductance pattern that is independent of the Mg concentration. The number of measured events is as follows: mock – 130 events, 2 mM Mg – 330 events, 4 mM – 127 events with peak conductance for mock at 25 nS, for 2 mM Mg at 20–25 nS and for 4 mM Mg at 25 nS. (C) Live-cell imaging analysis of mouse glial cell membrane permeabilization (as judged by PI staining) by  $4 \text{ HU} \cdot \text{mL}^{-1}$  PLY reveals delayed permeabilization and diminished number of permeabilized cells during treatment with 2 mM Mg. The curves are extrapolated beyond 120 min using non-linear regression curves fitted with one-phase exponential association ( $n = 5$  independent experiments). (D) Increased half-time of PLY permeabilization during treatment with 2 mM Mg ( $n = 5$  independent experiments). (E) Diminished permeabilization at the plateau of the regression curve in the presence of 2 mM Mg treatment ( $n = 5$  independent experiments). (F) Diminished LDH release by Mg at 60 min after PLY challenge, followed by equalized release at 6 h ( $n = 5$  independent experiments). \* $P < 0.05$ , significantly different as indicated; in (F), \* $P < 0.05$ , significant effect of Mg.

Information Figure S1B). Mice receiving  $MgCl_2$  had less severe clinical symptoms, that is, a lower clinical score, than infected mock animals (Figure 5C). Treatment with  $MgCl_2$

prolonged the survival of mice with pneumococcal meningitis significantly (Figure 5D). While in the group with mock-treated animals, eight (out of 19) succumbed to the infection

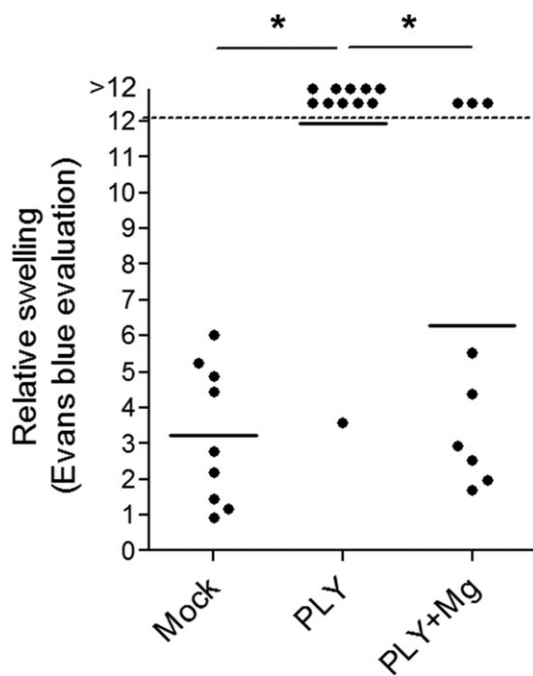


**Figure 4**

Effect of Mg on PLY brain oedema model in infant rats. The amount of Evans Blue (expressed as mm<sup>2</sup> after filter paper absorption) displaced out of the intracranial space (as a marker of elevated intracranial pressure) at 6 h after treatment with PLY (see Methods) in rats with or without treatment with MgCl<sub>2</sub> (500 mg·kg<sup>-1</sup> i.p.) at the beginning of the experiment, reveals ameliorated intracranial pressure increase after treatment with Mg<sup>2+</sup>. The intracranial pressure of the PLY-treated animals is significantly higher than that in the mock and PLY + Mg groups. Data shown are individual values with mean indicated by the horizontal line. \**P*<0.05, significantly different as indicated.

in the first 36 h after infection, only two (out of 18) mice treated with MgCl<sub>2</sub> died before the endpoint.

## Discussion

Our work demonstrates for the first time that clinically relevant concentrations of Mg<sup>2+</sup>, a well-known and established therapeutic agent, can prevent the brain pathogenicity of the neurotoxin PLY, which is released from *S. pneumoniae*, and provide a benefit for the outcome in animal models of pneumococcal meningitis.

Brain swelling, a complication of brain trauma, ischaemia, brain tumours and a variety of other disease conditions, contributes to lethality by compromising cerebral blood flow and/or by displacing important brain structures within the fixed volume of the skull (Marmarou, 2007; Raslan and Bhardwaj, 2007). The management of acute brain oedema in these cases is of primary clinical importance (Raslan and Bhardwaj, 2007). Brain swelling also plays a significant role in pneumococcal meningitis (Kastenbauer and Pfister, 2003; Brandt, 2010). Neuroinflammation and increased vascular permeability are considered major factors in infectious brain oedema (Stamatovic *et al.*, 2006). Earlier studies have

demonstrated that PLY can also produce intercellular oedema of the brain, widening the intercellular spaces and thus enhancing the tissue penetration of pathogenic factors and bacteria, because astrocyte reorganization plays a key role in this process (Hupp *et al.*, 2012).

The role of PLY as a critical pathogenic factor in pneumococcal meningitis has been confirmed in many experimental and clinical studies (Wellmer *et al.*, 2002; Reiß *et al.*, 2011; Wall *et al.*, 2012). Lack of PLY is associated with a much milder disease course and improved survival. Other members of the CDC toxin group such as perfringolysin and listeriolysin increase the virulence of their corresponding strains too (Bielecki *et al.*, 1990; Jones and Portnoy, 1994; Awad *et al.*, 2001). Immunization with PLY improves the survival rates of mice infected intranasally with *S. pneumoniae* (Paton *et al.*, 1983). Similarly, neutralizing antibodies against PLY improve the outcome after intranasal infection with *S. pneumoniae* and in PLY-induced lung injury (Salha *et al.*, 2012). These anti-PLY strategies, though effective, carry several practical therapeutic difficulties. Immunization with PLY is not an established, routine approach in patients and requires time until immunity is raised. The presence of the blood–brain and blood–CSF barrier complicates the penetration of therapeutic antibodies into the brain parenchyma and into the CSF (Neuwelt *et al.*, 1986; Gigliotti *et al.*, 1987), where bacteria accumulate in meningitis. In comparison, Mg<sup>2+</sup> represents a well-established, inexpensive and safe alternative that has proven effective for several clinical indications over many years. Magnesium is used in the treatment of eclampsia (Euser and Cipolla, 2009) and as an anti-arrhythmic agent in humans, with a daily dose as high as 600 mg·kg<sup>-1</sup> (Moran *et al.*, 1995). It is also neuroprotective and anti-oedematous in traumatic brain injury (van den Heuvel and Vink, 2004), although some newer meta-analyses caution against this conclusion (Li *et al.*, 2015). Magnesium lowers the incidence of death, cerebral palsy and motor dysfunction in preterm infants (Crowther *et al.*, 2003). In cases of intra-operative ischaemia during cardiac bypass and carotid endarterectomy, magnesium slows neurological decline at 24 h postoperatively (Bhudia *et al.*, 2006; Mack *et al.*, 2009), but some trials fail to replicate such effects (Mathew *et al.*, 2013). While most studies use magnesium in the form of MgSO<sub>4</sub> for historical reasons, we used MgCl<sub>2</sub>, which is considered to be pharmacologically comparable or even superior (Durlach *et al.*, 2005). The magnesium dose applied demonstrated the well-known side effect of muscle relaxation. This needs to be considered, especially in clinical cases with depressed breathing. Muscle relaxation tends to flatten breathing movements and thus can complicate anaesthesia in animal models.

We designed several experimental paradigms of treatment to identify the exact phase and mechanism of toxin/cell interaction modulated by magnesium. First, we pretreated brain tissue alone with magnesium before toxin challenge, evaluating some tissue-specific effects. Changes in membrane fluidity, for example, may affect the thermodynamic barrier to membrane penetration of the toxin and thus reduce the speed of pore formation (Nagahama *et al.*, 2007). The evidence that metal cations (including Mg<sup>2+</sup>) influence membrane fluidity in the brain and in platelets indeed supports such a mechanism (Ohba *et al.*, 1994; Sheu *et al.*,



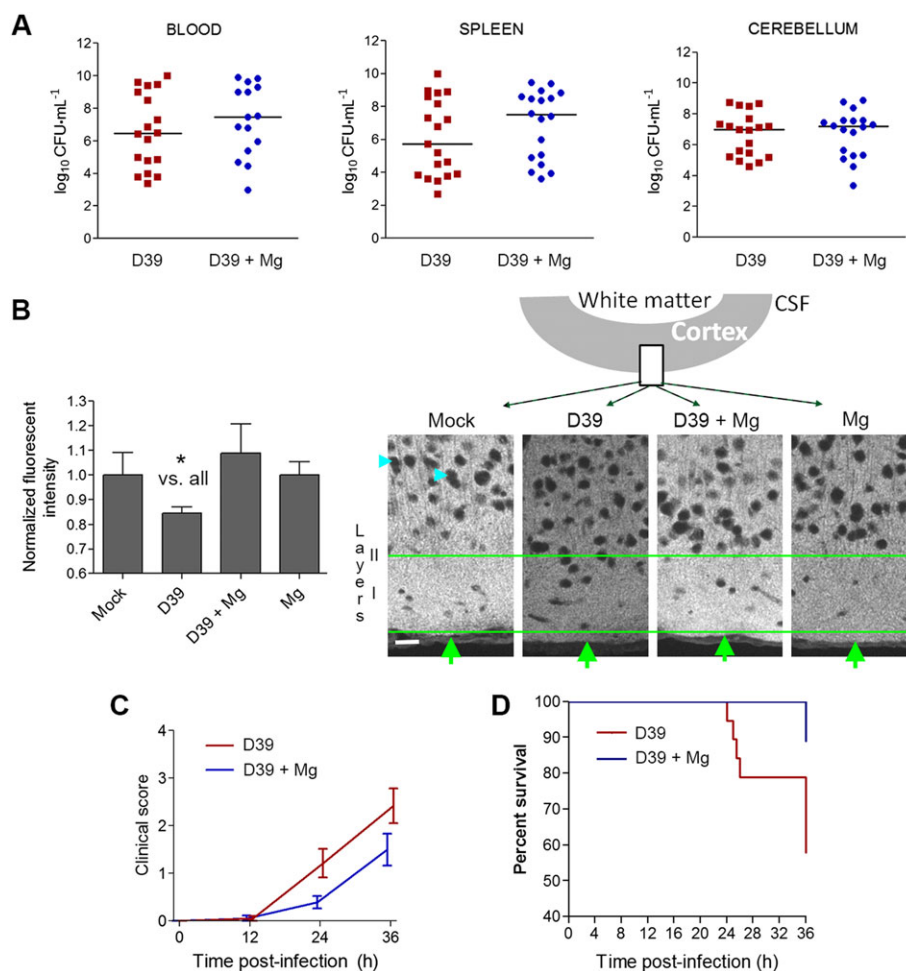


## Figure 5

Effect of magnesium treatment in mice with experimental *S. pneumoniae* D39 meningitis. (A) *S. pneumoniae* D39 concentrations (as CFUs) in blood, cerebellum and spleen homogenates after 36 h demonstrated comparable growth in infected mice treated i.p. with 0.45% NaCl (mock) or treated i.p. with  $\text{MgCl}_2$  (Mg). (B) Relative fluorescent intensity measurement of the PSD95 immunofluorescence in layers 1–3 of the neocortex at the level of the postcentral gyrus (mock ( $n = 4$  animals): NaCl-injected and NaCl-treated group; D39 ( $n = 19$  animals): Spn D39-infected and NaCl-treated group; D39 + Mg ( $n = 18$  animals): Spn D39-infected and  $\text{MgCl}_2$ -treated group; Mg ( $n = 3$  animals): NaCl-injected and  $\text{MgCl}_2$ -treated group) and corresponding fluorescent images (cyan arrows indicate staining-negative nuclear regions; green arrows – cortical surface; green lines limit the region of interest, including layer I and partially layer II; schematic diagram above indicates the position of the imaged fragment). Scale bar: 20  $\mu\text{m}$ . (C) Clinical score (0 = no apparent behavioural abnormality; 1, moderate lethargy; 2 = severe lethargy; 3 = unable to walk; 4 = dead) of the animals. Mock and Mg controls demonstrate score of 0 (not included in the graph, overlap with axis). For statistical analysis, the area under the curve is calculated and compared (see Methods). There was a significant effect of treatment with  $\text{Mg}^{2+}$ . (D) Survival curves of  $\text{MgCl}_2$  (Mg,  $n = 18$ ) or NaCl-treated (mock,  $n = 19$ ) infected animals. All mock and Mg controls demonstrate 100% survival at 36 h (not included in the graph, overlap of multiple lines). There was a significantly increased survival after treatment with  $\text{Mg}^{2+}$ .

2002). Tissue pretreatment with  $\text{Mg}^{2+}$  alone, however, was not effective against a subsequent PLY challenge, excluding to a large degree, direct tissue-conditioning effects. Much more informative were our experiments with toxin pre-incubation with  $\text{Mg}^{2+}$  and subsequent tissue toxin challenge in base medium conditions. Here, the effects of  $\text{Mg}^{2+}$  were substantially preserved, indicating longer-lasting effects of the metal ion on the toxin molecule. Some divalent cations, such as  $\text{Ca}^{2+}$  and  $\text{Zn}^{2+}$ , have the capacity to inhibit the binding of PLY to membranes (Beurg *et al.*, 2005; Franco-Vidal *et al.*, 2008). In contrast,  $\text{Mg}^{2+}$  did not inhibit the membrane binding of PLY as assessed by Western blot analysis. Another explanation of our results points to  $\text{Mg}^{2+}$  as a toxin

modulator agent after membrane binding, but the electrophysiological experiments did not provide evidence for changed toxin pore properties on the single pore level, as the peaks of conductance remained unchanged.

In the mixed glial cell culture system, treatment with  $\text{Mg}^{2+}$  delayed permeabilization in the first few hours after toxin challenge. At 6 h, however, lysis in all PLY-treated groups was equal. Comparative interpretation of the data from dissociated cell cultures and tissues is difficult as tissues contain extracellular matrix and complex cellular composition not present in cultures. The real advantage of the cell culture system, combined with live imaging, was the ability to study pore formation kinetics by PLY. There are several

possible explanations for the delay of permeabilization by  $Mg^{2+}$ : (i)  $Mg^{2+}$ -altered membrane turnover in the cells or (ii)  $Mg^{2+}$ -affected pore assembly. The experiments involving pretreatment with  $Mg^{2+}$  of slices and later addition of toxin indicated that the effects are mostly confined to the presence of toxin, supporting the second explanation. Interestingly, maintaining a high intracellular  $Mg^{2+}$  concentration represents a protective mechanism against autolysis in *S. pneumoniae* (Neef *et al.*, 2011).

Higher calcium concentrations mildly ameliorated swelling in our brain slice system (Supporting Information Figure S1C). The mechanisms involved here was most likely associated with the modulation of membrane toxin binding by calcium (Wippel *et al.*, 2011). High calcium, however, is not an alternative to the magnesium treatment due to the multiple secondary calcium-mediated effects such as enhanced cell dysfunction, excitotoxicity and accelerated cell death (Amagasa *et al.*, 1990; Ravens *et al.*, 1992; McGinnis *et al.*, 1999; Lorget *et al.*, 2000), but it further confirms the critical sensitivity of the PLY molecule to divalent ions. We hypothesize that at non-lytic, pro-oedematous PLY concentrations in slices,  $Mg^{2+}$ -induced delay of pore formation allows better tissue adaptation.

Pharmacologically, magnesium inhibits intracellular calcium influx *via* endogenous calcium channels (Iseri and French, 1984) and blocks the **NMDA receptors** of the brain, which are involved pathogenically in many disease conditions. Experiments demonstrate a role for glutamate release by PLY in producing synaptic dysfunction (Wippel *et al.*, 2013). We have shown before that the NMDA inhibition by MK-801 and AP5 does not alter the tissue swelling and astrocyte remodelling induced by PLY (Hupp *et al.*, 2012). Indeed, treatment with  $Mg^{2+}$  inhibited the decrease of PSD95 in the brains of animals with pneumococcal meningitis here, as the antagonizing effect may be attributed both to the antagonism of NMDA signalling and to the delayed PLY effect, but only regarding synaptic loss and not brain swelling. Apoptotic neuronal injury in meningitis (judged by active caspase-3 staining in the CA2 area of the hippocampus and in the neocortex) was not significantly altered, which can be explained with the nature of the mouse model we used – all mice die without antibiotic treatment within 72 h, and some researchers consider it not sensitive enough (Liechti *et al.*, 2015). On the other hand, this model is more reproducible and the groups are clinically more homogeneous, which allows for smaller experimental groups and more reliable statistics. The important finding here, however, was that treatment with  $Mg^{2+}$  prolonged the survival of infected animals without antibiotic treatment. Considering the anti-oedematous effect of  $Mg^{2+}$  against PLY and the fact that brain oedema is the major cause of mortality in young adults with meningitis (Koedel *et al.*, 2002), we believe that the enhanced survival is mostly a consequence of the reduction of brain swelling.

Calcium influx in cells in response to PLY exposure has been already demonstrated (Stringaris *et al.*, 2002; Wippel *et al.*, 2011). It is possible that  $Mg^{2+}$  acts as a blocker of the toxin-mediated calcium influx *via* pores, as it does so in many tissues by blocking endogenous calcium channels (Iseri and French, 1984). Here, however, we would expect certain changes in the conductance profile of PLY by  $Mg^{2+}$  in black

lipid membranes, even in the absence of calcium (Neuhaus and Cachelin, 1990), that we did not observe.

In considering the therapeutic application of magnesium, some authors have noted a variable pharmacological delivery of  $Mg^{2+}$  to the brain (Sun *et al.*, 2009), which does not always correspond to the serum levels after peripheral application. We suggest that this variability might explain the lack of a protective effect against PLY-induced oedema in some of the animals (3 out of 9). In the case of full-scale bacterial meningitis, however, the breakdown of the blood–brain barrier may prove useful by facilitating the delivery of  $Mg^{2+}$  into the brain.

In summary, we demonstrate that magnesium, a widely and safely used drug, could be an effective adjuvant therapeutic approach for pneumococcal meningitis together with other established therapies. To our knowledge, this is the first example of a clinically applicable compound that is capable of inhibiting, in therapeutic doses, the deleterious effects of a CDC. Our results would encourage the use of  $MgCl_2$  as an adjunct to antibiotic treatment in an appropriate animal model and, when positive results are obtained, to be followed by a clinical study in patients with bacterial meningitis.

## Acknowledgements

The work in Bern was funded by the Schweizerischer Nationalfonds zur Förderung der Wissenschaftlichen Forschung (SNF) (grant 31003A\_160136/1 to A.I.) and the University of Bern. The work in Göttingen was supported by the Deutsche Forschungsgemeinschaft (DFG) and Sparkasse Göttingen. The work in Würzburg was funded by the Emmy Noether Program of the Deutsche Forschungsgemeinschaft (DFG) (grant to A.I. IL-151.1), the Rudolf Virchow Center for Experimental Medicine, Würzburg, and the University of Würzburg. The work in Glasgow and Birmingham was supported by the Wellcome Trust (WT094762MA) and the European Science Foundation. We are grateful to Alexandra Bohl for excellent technical assistance.

## Author contributions

A.I., R.N. and R.B. worked on experimental design; S.H., S.R., J.S., C.B., C.F., E.M., A.I. and R.N. performed the experiments; S.H., S.R., J.S. and E.M. analysed the data; S.H., S.R., J.S., A.I., R.N., R.B. and T.M. wrote the manuscript; and T.M. provided the materials.

## Conflict of interest

The authors declare no conflicts of interest.

## Declaration of transparency and scientific rigour

This Declaration acknowledges that this paper adheres to the principles for transparent reporting and scientific rigour of preclinical research recommended by funding agencies,

publishers and other organisations engaged with supporting research.

## References

- Alexander SPH, Peters JA, Kelly E, Marrion N, Benson HE, Faccenda E *et al.* (2015a). The Concise Guide to PHARMACOLOGY 2015/16: Ligand-gated ion channels. *Br J Pharmacol* 172: 5870–5903.
- Alexander SPH, Fabbro D, Kelly E, Marrion N, Peters JA, Benson HE *et al.* (2015b). The Concise Guide to PHARMACOLOGY 2015/16: Enzymes. *Br J Pharmacol* 172: 6024–6109.
- Alouf JE (2000). Cholesterol-binding cytolytic protein toxins. *Int J Med Microbiol* 290: 351–356.
- Amagasa M, Ogawa A, Yoshimoto T (1990). Effects of calcium and calcium antagonists against deprivation of glucose and oxygen in guinea pig hippocampal slices. *Brain Res* 526: 1–7.
- Awad MM, Ellemor DM, Boyd RL, Emmins JJ, Rood JI (2001). Synergistic effects of alpha-toxin and perfringolysin O in *Clostridium perfringens*-mediated gas gangrene. *Infect Immun* 69: 7904–7910.
- Benz R, Janko K, Boos W, Lauger P (1978). Formation of large, ion-permeable membrane channels by the matrix protein (porin) of *Escherichia coli*. *Biochim Biophys Acta* 511: 305–319.
- Benz R, Ishii J, Nakae T (1980). Determination of ion permeability through the channels made of porins from the outer membrane of *Salmonella typhimurium* in lipid bilayer membranes. *J Membr Biol* 56: 19–29.
- Beurg M, Hafidi A, Skinner L, Cowan G, Hondarrague Y, Mitchell TJ *et al.* (2005). The mechanism of pneumolysin-induced cochlear hair cell death in the rat. *J Physiol* 568: 211–227.
- Bhudia SK, Cosgrove DM, Naugle RI, Rajeswaran J, Lam BK, Walton E *et al.* (2006). Magnesium as a neuroprotectant in cardiac surgery: a randomized clinical trial. *J Thorac Cardiovasc Surg* 131: 853–861.
- Bielecki J, Youngman P, Connelly P, Portnoy DA (1990). *Bacillus subtilis* expressing a haemolysin gene from *Listeria monocytogenes* can grow in mammalian cells. *Nature* 345: 175–176.
- Blanga-Kanfi S, Miranda H, Penn O, Pupko T, DeBry RW, Huchon D (2009). Rodent phylogeny revised: analysis of six nuclear genes from all major rodent clades. *BMC Evol Biol* 9: 71.
- Brandt CT (2010). Experimental studies of pneumococcal meningitis. *Dan Med Bull* 57: B4119.
- Canvin JR, Marvin AP, Sivakumaran M, Paton JC, Boulnois GJ, Andrew PW *et al.* (1995). The role of pneumolysin and autolysin in the pathology of pneumonia and septicemia in mice infected with a type 2 pneumococcus. *J Infect Dis* 172: 119–123.
- Crowther CA, Hiller JE, Doyle LW, Haslam RR (2003). Effect of magnesium sulfate given for neuroprotection before preterm birth: a randomized controlled trial. *JAMA* 290: 2669–2676.
- Curtis MJ, Bond RA, Spina D, Ahluwalia A, Alexander SP, Gjembycz MA *et al.* (2015). Experimental design and analysis and their reporting: new guidance for publication in BJP. *Br J Pharmacol* 172: 3461–3471.
- Denayer T, Stöhr T, Van Roy M (2014). Animal models in translational medicine: Validation and prediction. *New Horizons in Translational Medicine* 2: 5–11.
- Douce G, Ross K, Cowan G, Ma J, Mitchell TJ (2010). Novel mucosal vaccines generated by genetic conjugation of heterologous proteins to pneumolysin (PLY) from *Streptococcus pneumoniae*. *Vaccine* 28: 3231–3237.
- Durlach J, Guiet-Bara A, Pages N, Bac P, Bara M (2005). Magnesium chloride or magnesium sulfate: a genuine question. *Magnes Res* 18: 187–192.
- Euser AG, Cipolla MJ (2009). Magnesium sulfate for the treatment of eclampsia: a brief review. *Stroke* 40: 1169–1175.
- Flecknell P. (2002). Replacement, reduction and refinement. *Altex* 19: 73–78.
- Franco-Vidal V, Beurg M, Darrouzet V, Bebear JP, Skinner LJ, Dulon D (2008). Zinc protection against pneumolysin toxicity on rat cochlear hair cells. *Audiol Neurootol* 13: 65–70.
- Gerber J, Raivich G, Wellmer A, Noeske C, Kunst T, Werner A *et al.* (2001). A mouse model of *Streptococcus pneumoniae* meningitis mimicking several features of human disease. *Acta Neuropathol* 101: 499–508.
- Gigliotti F, Lee D, Insel RA, Scheld WM (1987). IgG penetration into the cerebrospinal fluid in a rabbit model of meningitis. *J Infect Dis* 156: 394–398.
- Grandgirard D, Leib SL (2010). Meningitis in neonates: bench to bedside. *Clin Perinatol* 37: 655–676.
- Grandgirard D, Burri M, Agyeman P, Leib SL (2012). Adjunctive daptomycin attenuates brain damage and hearing loss more efficiently than rifampin in infant rat pneumococcal meningitis. *Antimicrob Agents Chemother* 56: 4289–4295.
- van den Heuvel C, Vink R (2004). The role of magnesium in traumatic brain injury. *Clin Calcium* 14: 9–14.
- Hupp S, Heimeroth V, Wippel C, Fortsch C, Ma J, Mitchell TJ *et al.* (2012). Astrocytic tissue remodeling by the meningitis neurotoxin pneumolysin facilitates pathogen tissue penetration and produces interstitial brain edema. *Glia* 60: 137–146.
- Iliev AI, Stringaris AK, Nau R, Neumann H (2004). Neuronal injury mediated via stimulation of microglial toll-like receptor-9 (TLR9). *FASEB J* 18: 412–414.
- Iliev AI, Djannatian JR, Nau R, Mitchell TJ, Wouters FS (2007). Cholesterol-dependent actin remodeling via RhoA and Rac1 activation by the *Streptococcus pneumoniae* toxin pneumolysin. *Proc Natl Acad Sci U S A* 104: 2897–2902.
- Iliev AI, Djannatian JR, Opazo F, Gerber J, Nau R, Mitchell TJ *et al.* (2009). Rapid microtubule bundling and stabilization by the *Streptococcus pneumoniae* neurotoxin pneumolysin in a cholesterol-dependent, non-lytic and Src-kinase dependent manner inhibits intracellular trafficking. *Mol Microbiol* 71: 461–477.
- Iseri LT, French JH (1984). Magnesium: nature's physiologic calcium blocker. *Am Heart J* 108: 188–193.
- Jones S, Portnoy DA (1994). Characterization of *Listeria monocytogenes* pathogenesis in a strain expressing perfringolysin O in place of listeriolysin O. *Infect Immun* 62: 5608–5613.
- Kastenbauer S, Pfister HW (2003). Pneumococcal meningitis in adults: spectrum of complications and prognostic factors in a series of 87 cases. *Brain* 126: 1015–1025.
- Kilkenny C, Browne W, Cuthill IC, Emerson M, Altman DG (2010). Animal research: reporting *in vivo* experiments: the ARRIVE guidelines. *Br J Pharmacol* 160: 1577–1579.
- Koedel U, Scheld WM, Pfister HW (2002). Pathogenesis and pathophysiology of pneumococcal meningitis. *Lancet Infect Dis* 2: 721–736.

- Li W, Bai YA, Li YJ, Liu KG, Wang MD, Xu GZ *et al.* (2015). Magnesium sulfate for acute traumatic brain injury. *J Craniofac Surg* 26: 393–398.
- Liechti FD, Grandgirard D, Leib SL (2015). Bacterial meningitis: insights into pathogenesis and evaluation of new treatment options: a perspective from experimental studies. *Future Microbiol* 10: 1195–1213.
- Lorget F, Kamel S, Mentaverri R, Wattel A, Naassila M, Maamer M *et al.* (2000). High extracellular calcium concentrations directly stimulate osteoclast apoptosis. *Biochem Biophys Res Commun* 268: 899–903.
- Mack WJ, Kellner CP, Sahlein DH, Ducruet AF, Kim GH, Mocco J *et al.* (2009). Intraoperative magnesium infusion during carotid endarterectomy: a double-blind placebo-controlled trial. *J Neurosurg* 110: 961–967.
- Marmarou A (2007). A review of progress in understanding the pathophysiology and treatment of brain edema. *Neurosurg Focus* 22: E1.
- Mathew JP, White WD, Schinderle DB, Podgoreanu MV, Berger M, Milano CA *et al.* (2013). Intraoperative magnesium administration does not improve neurocognitive function after cardiac surgery. *Stroke* 44: 3407–3413.
- McGinnis KM, Wang KK, Gnegy ME (1999). Alterations of extracellular calcium elicit selective modes of cell death and protease activation in SH-SY5Y human neuroblastoma cells. *J Neurochem* 72: 1853–1863.
- McGrath JC, Lilley E (2015). Implementing guidelines on reporting research using animals (ARRIVE etc.): new requirements for publication in BJP. *Br J Pharmacol* 172: 3189–3193.
- Moran JL, Gallagher J, Peake SL, Cunningham DN, Salagaras M, Leppard P (1995). Parenteral magnesium sulfate versus amiodarone in the therapy of atrial tachyarrhythmias: a prospective, randomized study. *Crit Care Med* 23: 1816–1824.
- Nagahama M, Otsuka A, Oda M, Singh RK, Ziara ZM, Imagawa H *et al.* (2007). Effect of unsaturated bonds in the sn-2 acyl chain of phosphatidylcholine on the membrane-damaging action of Clostridium perfringens alpha-toxin toward liposomes. *Biochim Biophys Acta* 1768: 2940–2945.
- Nau R, Wellmer A, Soto A, Koch K, Schneider O, Schmidt H *et al.* (1999). Rifampin reduces early mortality in experimental *Streptococcus pneumoniae* meningitis. *J Infect Dis* 179: 1557–1560.
- Neef J, Andisi VF, Kim KS, Kuipers OP, Bijlsma JJ (2011). Deletion of a cation transporter promotes lysis in *Streptococcus pneumoniae*. *Infect Immun* 79: 2314–2323.
- Neuhaus R, Cachelin AB (1990). Changes in the conductance of the neuronal nicotinic acetylcholine receptor channel induced by magnesium. *Proceedings Biological sciences / The Royal Society* 241: 78–84.
- Neuwelt EA, Specht HD, Hill SA (1986). Permeability of human brain tumor to 99mTc-gluco-heptonate and 99mTc-albumin. Implications for monoclonal antibody therapy. *J Neurosurg* 65: 194–198.
- O'Hara J (2008). How I do it: sample size calculations. *Clin Otolaryngol* 33: 145–149.
- Ohba S, Hiramatsu M, Edamatsu R, Mori I, Mori A (1994). Metal ions affect neuronal membrane fluidity of rat cerebral cortex. *Neurochem Res* 19: 237–241.
- Paton JC, Lock RA, Hansman DJ (1983). Effect of immunization with pneumolysin on survival time of mice challenged with *Streptococcus pneumoniae*. *Infect Immun* 40: 548–552.
- Raslan A, Bhardwaj A (2007). Medical management of cerebral edema. *Neurosurg Focus* 22: E12.
- Ravens U, Liu GS, Vandeplasse G, Borgers M (1992). Protection of human, rat, and guinea-pig atrial muscle by miflozine, lidoflazine, and verapamil against the destructive effects of high concentrations of Ca<sup>2+</sup>. *Cardiovasc Drugs Ther* 6: 47–58.
- Reiß A, Braun JS, Jäger K, Freyer D, Laube G, Bühner C *et al.* (2011). Bacterial pore-forming cytolysins induce neuronal damage in a rat model of neonatal meningitis. *Journal of Infectious Diseases* 203: 393–400.
- Salha D, Szeto J, Myers L, Claus C, Sheung A, Tang M *et al.* (2012). Neutralizing antibodies elicited by a novel detoxified pneumolysin derivative, PlyD1, provide protection against both pneumococcal infection and lung injury. *Infect Immun* 80: 2212–2220.
- Sheu JR, Hsiao G, Shen MY, Fong TH, Chen YW, Lin CH *et al.* (2002). Mechanisms involved in the antiplatelet activity of magnesium in human platelets. *Br J Haematol* 119: 1033–1041.
- Southan C, Sharman JL, Benson HE, Faccenda E, Pawson AJ, Alexander SPH *et al.* (2016). The IUPHAR/BPS guide to PHARMACOLOGY in 2016: towards curated quantitative interactions between 1300 protein targets and 6000 ligands. *Nucl Acids Res* 44: D1054–D1068.
- Spreer A, Kerstan H, Bottcher T, Gerber J, Siemer A, Zysk G *et al.* (2003). Reduced release of pneumolysin by *Streptococcus pneumoniae* in vitro and in vivo after treatment with nonbacteriolytic antibiotics in comparison to ceftriaxone. *Antimicrob Agents Chemother* 47: 2649–2654.
- Stamatovic SM, Dimitrijevic OB, Keep RF, Andjelkovic AV (2006). Inflammation and brain edema: new insights into the role of chemokines and their receptors. *Acta Neurochir Suppl* 96: 444–450.
- Stringaris AK, Geisenhainer J, Bergmann F, Balshusemann C, Lee U, Zysk G *et al.* (2002). Neurotoxicity of pneumolysin, a major pneumococcal virulence factor, involves calcium influx and depends on activation of p38 mitogen-activated protein kinase. *Neurobiol Dis* 11: 355–368.
- Sun L, Kosugi Y, Kawakami E, Piao YS, Hashimoto T, Oyanagi K (2009). Magnesium concentration in the cerebrospinal fluid of mice and its response to changes in serum magnesium concentration. *Magn Res* 22: 266–272.
- Tengvar C, Forssen M, Hultstrom D, Olsson Y, Pertoft H, Pettersson A (1982). Measurement of edema in the nervous system. Use of Percoll density gradients for determination of specific gravity in cerebral cortex and white matter under normal conditions and in experimental cytotoxic brain edema. *Acta Neuropathol* 57: 143–150.
- Tilley SJ, Orlova EV, Gilbert RJ, Andrew PW, Saibil HR (2005). Structural basis of pore formation by the bacterial toxin pneumolysin. *Cell* 121: 247–256.
- Wall EC, Gordon SB, Hussain S, Goonetilleke UR, Gritzfeld J, Scarborough M *et al.* (2012). Persistence of pneumolysin in the cerebrospinal fluid of patients with pneumococcal meningitis is associated with mortality. *Clin Infect Dis* 54: 701–705.
- Wellmer A, Zysk G, Gerber J, Kunst T, Von Mering M, Bunkowski S *et al.* (2002). Decreased virulence of a pneumolysin-deficient strain of *Streptococcus pneumoniae* in murine meningitis. *Infect Immun* 70: 6504–6508.
- Wippel C, Fortsch C, Hupp S, Maier E, Benz R, Ma J *et al.* (2011). Extracellular calcium reduction strongly increases the lytic capacity of pneumolysin from *Streptococcus pneumoniae* in brain tissue. *J Infect Dis* 204: 930–936.
- Wippel C, Maurer J, Förtsch C, Hupp S, Bohl A, Ma J *et al.* (2013). Bacterial cytolysin during meningitis disrupts the regulation of glutamate in the brain, leading to synaptic damage. *PLoS Pathog* 9: e1003380.

## Supporting Information

Additional Supporting Information may be found online in the supporting information tab for this article.

<https://doi.org/10.1111/bph.14027>

**Figure S1** Additional information. A. Weight loss in mouse meningitis experimental groups at the end of the experiment. No significant differences between individual groups

are observed. B. Active caspase 3 cells in the CA2 region of the mouse hippocampus. No significant differences among groups were observed despite tendency towards increased number of active caspase-3 positive cells in the D39-group. C. 2 mM additional calcium (in the form of  $\text{CaCl}_2$ ) inhibited mildly brain slice swelling by 4 HU/ml PLY ( $n = 4$  independent experiments).

**Figure S2** Original Western blots with anti-pneumolysin (anti-PLY) staining of membrane fractions and normalization signals with cytosolic actin (anti-actin) detection.